Dynamic Power Analysis of Inverter-Fed Drives based on the Switching Period of the Power Electronics

Alexander Stock
Hottinger Brüel & Kjær GmbH
Im Tiefen See 45
64293 Darmstadt, Germany
Email: alexander.stock@hbkworld.com
URL: https://www.hbkworld.com

Keywords

≪Measurements≫, ≪Variable speed drive≫, ≪Pulsed power converter≫, ≪Pulse Width Modulation (PWM)≫, ≪Real-time processing≫

Abstract

Maximizing efficiency is one of the key design criteria for inverter-fed drives. The basis of this optimization process is a reliable measurement of the efficiency. The efficiency determination is in turn based on the cyclic calculation of the active power quantities based the fundamental period of the electrical quantities (voltages and currents) which is defined in detail in the relevant standards. For this reason, periodic voltages and currents are assumed to result in a steady-state condition of the drive if the standards are interpreted accurately. In many modern, highly dynamic applications (automotive, robotics, etc.), however, steady-state conditions are rare during normal operation. The electrical quantities change continuously both in magnitude and frequency and are characterized by transient behavior. In this paper, a novel highly dynamic measurement method for the approximation of the active power and efficiency is presented with regard to these dynamic applications. This methodology still approximates the conventional fundamental cycle-based definitions in the steady state, but also delivers additional dynamic information during transient balancing processes. The dynamic power analysis uses the switching period of the power electronics as averaging interval. For this reason, with regard to real-time measurements, a robust online switching cycle detection is an essential requirement to be able to perform this power analysis on a real-time capable power analyzer.

Introduction

Many industrial applications, such as fan or pump drives, are mainly operated at steady-state conditions. On the other hand, the increase in performance in the area of control and information technology as well as the constantly increasing switching frequencies of new power semiconductors enable the realization of modern highly dynamic drive concepts. In this context, for example, the rapidly growing market of electromobility or applications in the field of robotics should be mentioned. In these latter applications, the drives are hardly operated in steady states. The operating points in such dynamic applications change very frequently and often continuously. Therefore, it is essential to be able to measure and evaluate the efficiency and losses of these drives in non-steady-state operation, both during the development process and in everyday use.

The loss or efficiency determination is regulated in relevant standards, see [1] just to mention one of several examples. The basis for the efficiency calculation is the active power, which represents the average energy transport per fundamental period related to this period length. It is calculated as the average of the instantaneous power over the fundamental cycle of the associated phase voltages and phase currents

of the investigated drive, see standards [2, 3, 4]. If these standards are interpreted accurately, all definitions of active power refer to the period of the periodic voltages and currents. However, the voltages and currents of the previously mentioned highly dynamic drives in automotive or robotics are non-periodic signals, characterized by transient peaks and continuously varying frequency and amplitude. In practice, the definitions and procedures of the standards can also be applied to these dynamic signals. In this case the averaging interval may be determined by a zero crossing detection or phase locked loop (PLL) circuits. Since there are no periodic signals at all, the averaging interval determined in this way cannot represent the fundamental period.

This paper presents methods for determining novel power quantities that result from averaging over the switching period of the inverter instead of the fundamental period. These power quantities approximate the conventional definitions from the relevant standards during the steady state and combine them in a new power quantity, additionally including transient information from instantaneous quantities during balancing processes, see [5, 6, 7]. In this context, to mention an example, the dynamic active power is introduced as an approximation of the conventional active power during steady state. However, this dynamic active power additionally contains information of the instantaneous power during transient balancing processes. This method can be extended to several other averaged power quantities, fundamental quantities, RMS values, see [6, 7, 8]. To be able to perform this analysis on a real-time power analyzer, a robust online switching cycle detection is essential. This paper presents the methodology of the dynamic power analysis. Comparative measurements are used to illustrate the advantages of these dynamic definitions. Finally, it is shown how the measurement process of an efficiency mapping may be drastically accelerated by use of this novel analysis method.

Dynamic power analysis

Time domain approach

Fig. 1 shows a general abstracted equivalent circuit diagram of a n-phase system as it is typically used for power analysis according to [6, 7, 9, 10, 11].

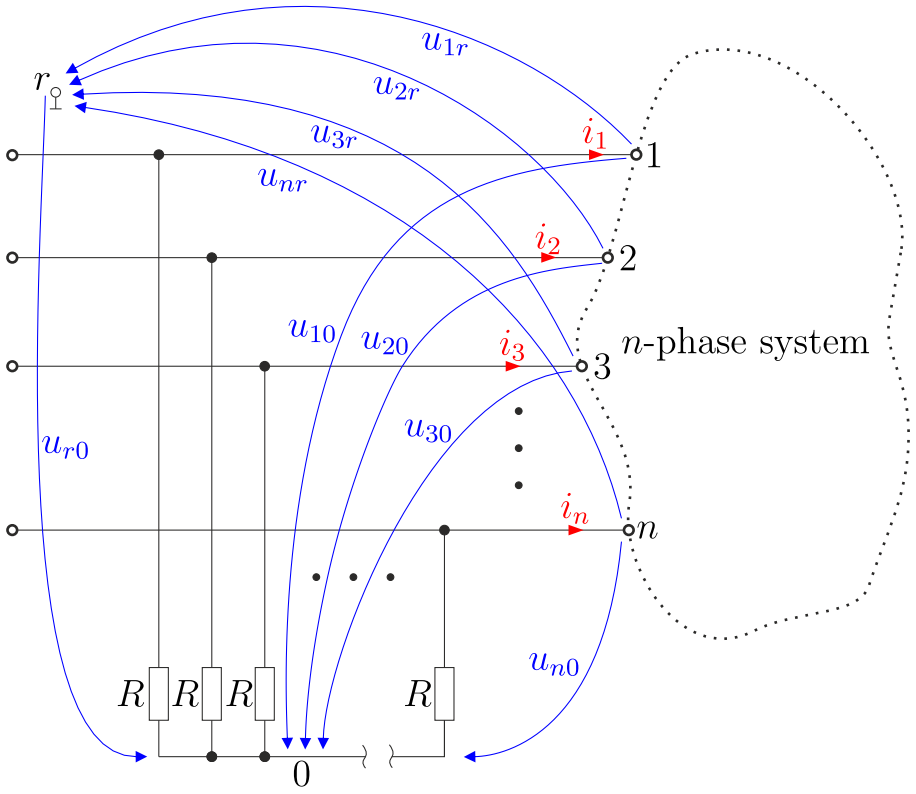

Fig. 1: Abstracted equivalent circuit diagram of an n-phase system as used for power analysis [6]

All conductor voltages and currents connected to the n-phase system and contributing to the power transfer must be considered in the power analysis [6, 10, 11] (but not the communication lines or protective earth conductors, etc.). The power analysis is completely defined by the terminal behavior of the measured system whereas the internal system topology is irrelevant for the power analysis of the total system. The voltages may be measured in theory against any arbitrary reference potential r resulting in $u_{1r}, u_{2r}, \ldots, u_{nr}$. In practice, of course, the reference potential should be galvanically connected to the measured circuit (e.g., ground potential, star point of an electric machine, artificial star point, negative DC link potential, etc.). Since the sum of the measured phase currents is zero due to Kirchhoff's law, the zero system voltage $u_{0r} = -u_{r0}$ can not carry a current and does therefore not contribute to the instantaneous power $p(t)$:

$$\begin{aligned} p(t) =& u_{1r} \cdot i_1 + u_{2r} \cdot i_1 + \cdots + u_{nr} \cdot i_n = (u_{10} + u_{0r}) \cdot i_1 + (u_{20} + u_{0r}) \cdot i_1 + \cdots + (u_{n0} + u_{0r}) \cdot i_n \\ =& u_{10} \cdot i_1 + u_{20} \cdot i_1 + \cdots + u_{n0} \cdot i_n + u_{0r} \cdot \underbrace{(i_1 + i_2 + \cdots + i_n)}_{=0} = u_{10} \cdot i_1 + u_{20} \cdot i_1 + \cdots + u_{n0} \cdot i_n \end{aligned} \tag{1}$$

However, the zero system voltage affects on the RMS values and therefore also on reactive and apparent power quantities. Since the result of the power analysis should be defined exclusively by the terminal behavior of the investigated system and therefore must not depend on the reference potential of the voltage measurement, the zero system voltage should always be subtracted first. Power analysis should be performed using the natural-zero-voltages $u_{10}, u_{20}, \ldots, u_{n0}$ only:

$$u_{\nu 0}(t) = u_{\nu r}(t) - u_{0r} \qquad \text{with} \qquad u_{0r} = \frac{1}{n} \cdot \sum_{\mu=1}^{n} u_{\mu r} \qquad \text{for} \qquad \nu \in \{1, 2, \ldots, n\} \tag{2}$$

According to the relevant standards [2, 3, 4] and technical literature, e.g., [9, 10, 11], the active power P is defined as the time average of the instantaneous power $p(t)$ over the fundamental period T_{h1} of the associated periodic voltages $u_{\nu 0}$ and currents i_ν:

$$P = \overline{p(t)}\Big|_{T_{\mathrm{h1}}} = \frac{1}{T_{\mathrm{h1}}} \int_{T_{\mathrm{h1}}} p(\tau)\,\mathrm{d}\tau \tag{3}$$

The basic concept of dynamic active power P_{dyn} is to shorten the averaging interval from the fundamental period to the switching period of the inverter T_{s}:

$$P_{\mathrm{dyn}} = \overline{p(t, T_{\mathrm{s}})}\Big|_{T_{\mathrm{s}}} = \frac{1}{T_{\mathrm{s}}} \int_{T_{\mathrm{s}}} p(\tau, T_{\mathrm{s}})\,\mathrm{d}\tau \tag{4}$$

The switching cycle is derived from the measured inverter voltages. For typical pulse-width modulated (PWM) inverter output voltages, this can result in an increase of the averaging frequency by a factor of up to a few hundreds (e.g., $f_{\mathrm{h1}} = 1/T_{\mathrm{h1}} = 50\,\mathrm{Hz}$, $f_{\mathrm{s}} = 1/T_{\mathrm{s}} = 8\,\mathrm{kHz} \Rightarrow f_{\mathrm{s}}/f_{\mathrm{h1}} = 160$). Furthermore, assuming that typical PWM-generated inverter output voltages are applied to a symmetrical ohmic-inductive 3-phase load during steady state (e.g., a 3-phase machine), the equivalence of the conventional active power definition and the dynamic active power definition could be shown in [6, 7] for the theoretical limit value consideration of an infinitesimal switching period, i.e. for $T_{\mathrm{s}} \to 0$ or $f_{\mathrm{s}} \to \infty$. Based on this derivation, it is further shown in [6] that the dynamic active power coincides exactly with the active power for the theoretical case of infinite switching frequency during steady state, if the instantaneous power is constant for this limit value consideration:

$$\lim_{T_\mathrm{s}\to 0}\left[P_\mathrm{dyn}\right] = P \quad \text{for} \quad \lim_{T_\mathrm{s}\to 0}\left[p(t,T_\mathrm{s})\right] = p(t) = \text{const} = p = P \tag{5}$$

For real applications with limited (finite) switching frequency, the higher the switching frequency compared to the fundamental frequency, the better the quality of the approximation of the conventional active power by the dynamic active power during the steady state. The relative error ΔP_dyn can be used as indicator for a maximum tolerable deviation:

$$P_\mathrm{dyn} \approx P \quad \text{for} \quad T_\mathrm{s} \ll T_\mathrm{h1} \quad \text{so that} \quad \left|\frac{\overline{p(t,T_\mathrm{s})}\Big|_{T_\mathrm{s}} - P}{P}\right| \leq \Delta P_\mathrm{dyn} \tag{6}$$

Frequency domain consideration

The characteristics of the switching cycle-based active power can also be visualized in the frequency domain as function of the frequency f by applying a discrete Fourier transform (DFT) on sampled values of instantaneous power $p_k = p(kT_\mathrm{a})$ with the sample period T_a and $k \in \mathbb{N}$. The graphics of this subsection are based on simulated data. Fig. 2 shows, as an example, the amplitude spectrum $|\underline{\hat{p}}_\nu| = |\mathcal{DFT}\{p_k\}|$ of the total instantaneous power of a balanced ohmic-inductive 3-phase load operated with sinusoidal PWM (SPWM), as well as the amplitude response of a switching cycle-based averaging filter $|\underline{G}(\Omega)|$ with the sample frequency $f_\mathrm{a} = 1/T_\mathrm{a}$, the normalized angular frequency $\Omega = 2\pi\frac{f}{f_\mathrm{a}}$, and assuming an integer number of samples per switching period $N = f_\mathrm{a}/f_\mathrm{s}$ with $N \in \mathbb{N}$, see [6]:

$$|\underline{G}(\Omega)| = \frac{1}{N}\cdot\left|\frac{\sin\left(\frac{1}{2}N\Omega\right)}{\sin\left(\frac{1}{2}\Omega\right)}\right| = \frac{f_\mathrm{s}}{f_\mathrm{a}}\cdot\left|\frac{\sin\left(\pi\frac{f}{f_\mathrm{s}}\right)}{\sin\left(\pi\frac{f}{f_\mathrm{a}}\right)}\right| = |\underline{G}(f)| \tag{7}$$

In this example, the inductance of the load is assumed to be sufficiently large resulting in purely sinusoidal load currents, whose switching frequency harmonics are therefore neglected. The amplitude spectrum of the instantaneous power is normalized to the product of the fundamental voltage amplitude $\hat{u}$, the amplitude of the sinusoudal current $\hat{i}$ and the cosine of the phase shift angle $\cos(\varphi)$ between the fundamental voltage and current waveform.

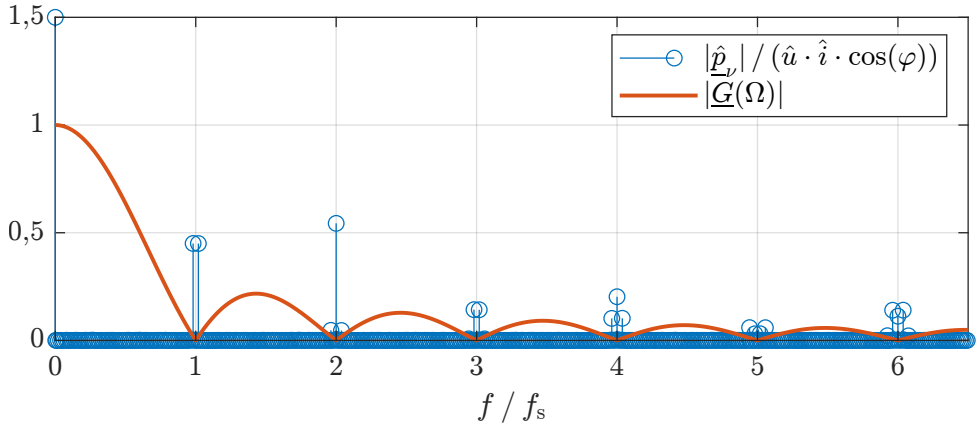

Fig. 2: Amplitude spectrum of the instantaneous power of a balanced ohmic-inductive 3-phase load fed by a SPWM-modulated inverter output voltage assuming a huge load inductance resulting in purely sinusoidal load currents [6]

Considering periodic voltages and currents, the active power P in (3), defined as fundamental cycle-based average of the instantaneous power $p(t)$, is thus represented by the DC-component of the instantaneous power. As it is well known from scientific literature, only corresponding harmonics of voltages and currents contribute to active power, resulting in $P = \frac{3}{2} \cdot \hat{u} \cdot \hat{i} \cdot \cos(\varphi)$, see [12], due to the purely sinusoidal currents. For this reason, as expected with regard to the normalization of the amplitude spectrum, $|\underline{\hat{p}}_0| = |\underline{\hat{p}}(f = 0 \cdot f_\mathrm{a})| = \frac{3}{2} = 1.5$, see Fig. 2.

Based on the definition in (4), the amplitude spectrum of the dynamic active power $|\underline{\hat{P}}_\mathrm{dynv}|$ can be calculated multiplying the amplitude spectrum of the instantaneous power $|\underline{\hat{p}}_\nu|$ by the amplitude response of the switching cycle-based average filter $|\underline{G}_\nu|$. For this, $|\underline{G}(\Omega)|$ is evaluated at discrete frequencies $\Omega = 2\pi\frac{\nu}{N-1}$ with $\nu \in \{0, 1, \ldots, N-1\}$ leading to $= |\underline{G}(2\pi\frac{\nu}{N-1})| = |\underline{G}_\nu|$:

$$|\underline{\hat{P}}_\mathrm{dynv}| = |\underline{G}_\nu| \cdot |\underline{\hat{p}}_\nu| \tag{8}$$

As expected from Fig. 2, with regard to (7), $\lim\limits_{f \to 0} |\underline{G}(f)| = 1$,see [6], whereas $|\underline{G}(f = k f_\mathrm{s})| = 0$, $k \in \mathbb{N}$. For this reason, $|\underline{\hat{P}}_\mathrm{dyn0}| = \frac{3}{2}$. For all $\nu \neq 0$, the harmonics $|\underline{\hat{P}}_\mathrm{dynv}|$ are strongly damped by at least a factor of approximately 100 compared to the DC-component, see Fig. 3:

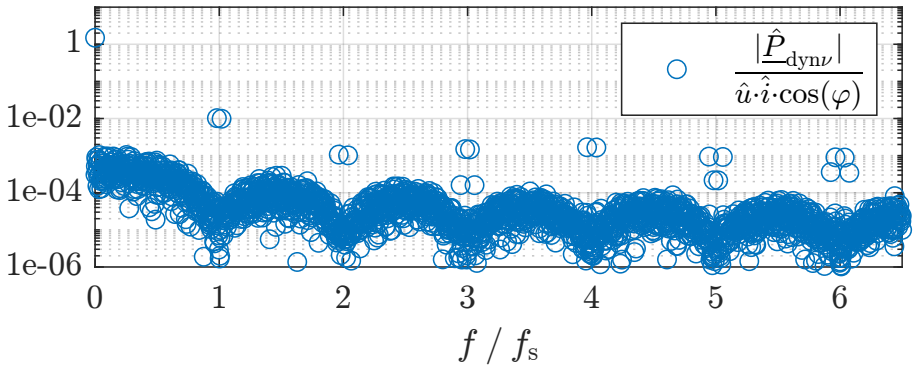

Fig. 3: Amplitude spectrum of dynamic active power normalized to its fundamental [6]

In addition to the DC component, integer multiples of the switching frequency and associated sidebands, i.e., integer multiples of the switching frequency plus/minus integer multiples of the fundamental frequency, occur in the amplitude spectrum of the instantaneous power in Fig. 2. It is obvious that the amplitudes of the sidebands decrease with increasing frequency gap from the switching frequency harmonics (related center frequencies). Therefore, when calculating the dynamic active power spectrum according to (8), these sidebands are strongly damped. Nevertheless, only the integer multiples of the switching frequency are completely eliminated by averaging. For this reason, the dynamic active power is in general not equal but a powerful approximation of the conventional active power during steady state.

If the switching frequency is increased while the fundamental frequency remains constant, the frequency gaps between the sidebands and the corresponding center frequencies (switching frequency harmonics) decrease with respect to the absolute value of the respective center frequencies. In this way, the harmonics in the sidebands are increasingly damped applying the switching cycle-based averaging filter. With regard to Fig. 2, continuing this argumentation graphically illustrates and reinforces the mathematical limit value consideration in (5). The switching frequency-based averaging for the theoretical case of an infinite switching frequency not only completely eliminates the integer multiples of the switching frequency, but also the associated sidebands. This is consistent with the mathematical time domain requirement (5): $\lim\limits_{T_\mathrm{s} \to 0} [p(t, T_\mathrm{s})] = \mathrm{const} \;\Rightarrow\; \lim\limits_{T_\mathrm{s} \to 0} \left[P_\mathrm{dyn}\right] = P$.

However, even at infinitely high switching frequency, the condition of constant instantaneous power must in general not always be fulfilled. In the following, an ohmic-inductive 2-pole system is considered instead of the 3-phase system. Assuming again a SPWM-generated inverter output voltage and a

purely sinusoidal current due to sufficiently large inductance, the resulting amplitude spectrum of the instantaneous power is depicted in Fig. 4.

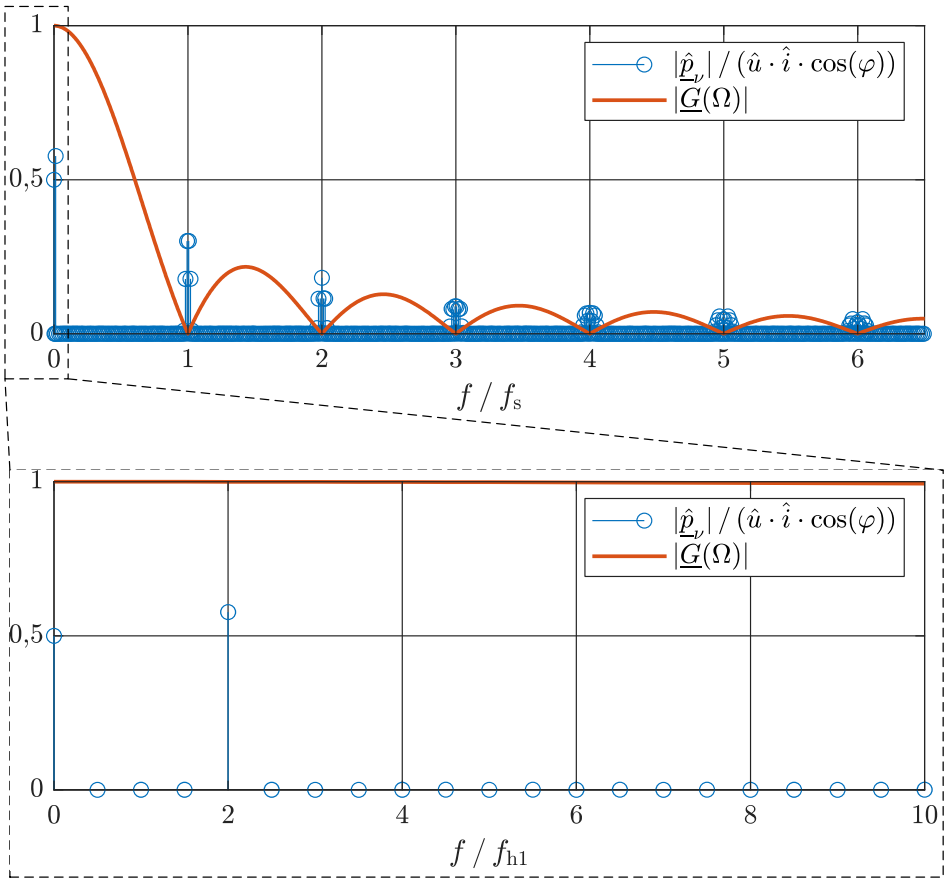

Fig. 4: Amplitude spectrum of the instantaneous power of an ohmic-inductive 2-pole load fed by a SPWM-modulated inverter output voltage assuming a huge load inductance resulting in purely sinusoidal load currents

It should be mentioned at first, that the zoomed bottom plot of Fig. 4 is normalized to the fundamental frequency f_h1, whereas the top plot is again normalized to the switching frequency in analogy to Fig. 2. Since only corresponding harmonics of voltages and currents contribute to active power, $P = \frac{1}{2}\cdot\hat{u}\cdot\hat{i}\cdot\cos(\varphi)$, the normalized DC component results in $|\underline{\hat{p}}_0| = \frac{1}{2} = 0.5$. However, in contrast to the 3-phase system, the amplitude spectrum of the instantaneous power in this case also contains the 2nd harmonic related to the fundamental $|\underline{\hat{p}}(f = 2f_\mathrm{h1})| = \frac{\hat{u}\hat{i}}{2}$, see [12]. However, the 2nd harmonic is not eliminated by averaging over the switching cycle. On the contrary, it is propagated to $|\underline{\hat{P}}_\mathrm{dynv}|$ due to the factor $|\underline{G}(f = 2f_\mathrm{h1})| \approx 1$. For this reason, the switching frequency-based averaging at the investigated two-pole system does not approximate the active power. It merely reflects the instantaneous power as it would occur using a purely sinusoidal supply voltage instead of a SPWM-modulated inverter.

Nevertheless, the dynamic power analysis based on the inverter's switching cycle is very suitable for PWM-operated inverter-fed multiphase systems ($n > 2$) as long as the switching frequency f_s is significantly higher than the fundamental frequency f_h1, typically at least $f_\mathrm{s} \geq 10 f_\mathrm{h1}$. The exact requirements furthermore depend on the applied PWM method and the individual load characteristics (e.g. current ripple or imbalances).

Comparative measurements

Startup process of a PMSM

In this section, comparative measurements of conventional fundamental cycle-based determination and dynamic switching cycle-based calculation methods are presented. In this way, the advantages of dynamic calculation can be illustrated.

First, a no-load start-up process of an double 2-level inverter-fed 3-phase permanent magnet synchronous machine (PMSM) is investigated. The system topology is shown in Fig. 5.

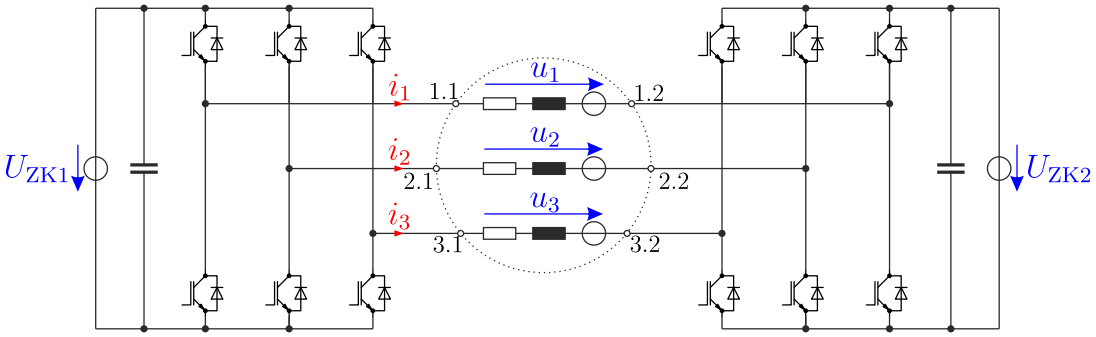

Fig. 5: Double 2-level inverter-fed PMSM[6]

The PMSM is accelerated from standstill to a constant steady state operating speed. During steady state, only the power loss must be supplied in order to control a constant speed. To accelerate the machine, torque generating currents must be injected by the inverter. The current in the first conductor i_1 is shown in the top plot of Fig. 6, normalized to the nominal current I_N of the PMSM. Based on the zero-crossings of this current, the corresponding fundamental period represented by the cycle signal CycleDetect(i_1) can be calculated on the measurement system in real-time. For reasons of causality, applying the conventional active power calculation from (3), the first active power value can be calculated as average over the fundamental period at the earliest after the complete detection of this period, i.e. after its end. The bottom plot in Fig. 6 shows the instantaneous power p, the (conventional) active power P and the dynamic active power P_{dyn}, each normalized to the product of the averaged DC-link voltage of the inverter system $U_{ZK} = \frac{U_{ZK1}+U_{ZK2}}{2}$ and the nominal current I_N.

With regard to (1), the instantaneous power contains the switching frequency harmonics predominantly affected by the inverter output voltages. The instantaneous power does not visually reflect any useful information about the average energy consumption of the PMSM during this start-up process. As described above, the conventional active power is delayed by one fundamental period during real-time measurements due to causality. For this reason, on a power meter or data acquisition system, the active power result could be calculated and visualized earliest during the following fundamental period, while the next active power value is determined simultaneously. A comparison of p and P shows that this method of active power calculation is not useful for this transient acceleration process, especially with regard to the real-time calculation of active power. With a precise interpretation of the relevant standards [1, 2, 3], the active power during this balancing process is not defined anyway due to aperiodic voltages and currents. On the other hand, the switching cycle can be detected by evaluating an inverter output voltage. The dynamic active power calculation in (4) is therefore only delayed by one switching period during real-time measurements. Based on Fig. 6, it is clear that P_{dyn} highly dynamically reflects the information about the average energy transfer per switching period.

At first glance, it seems theoretically obvious to achieve a similar dynamic active power result by simply low-pass filtering the instantaneous power using a first order low pass filter or even higher order. However, there are reasonable arguments to perform the switching cycle-based averaging. For example, if a fundamental period contains N switching periods, a subsequent average over the N already averaged dynamic active power results delivers exactly the same result as directly applying the conventional active

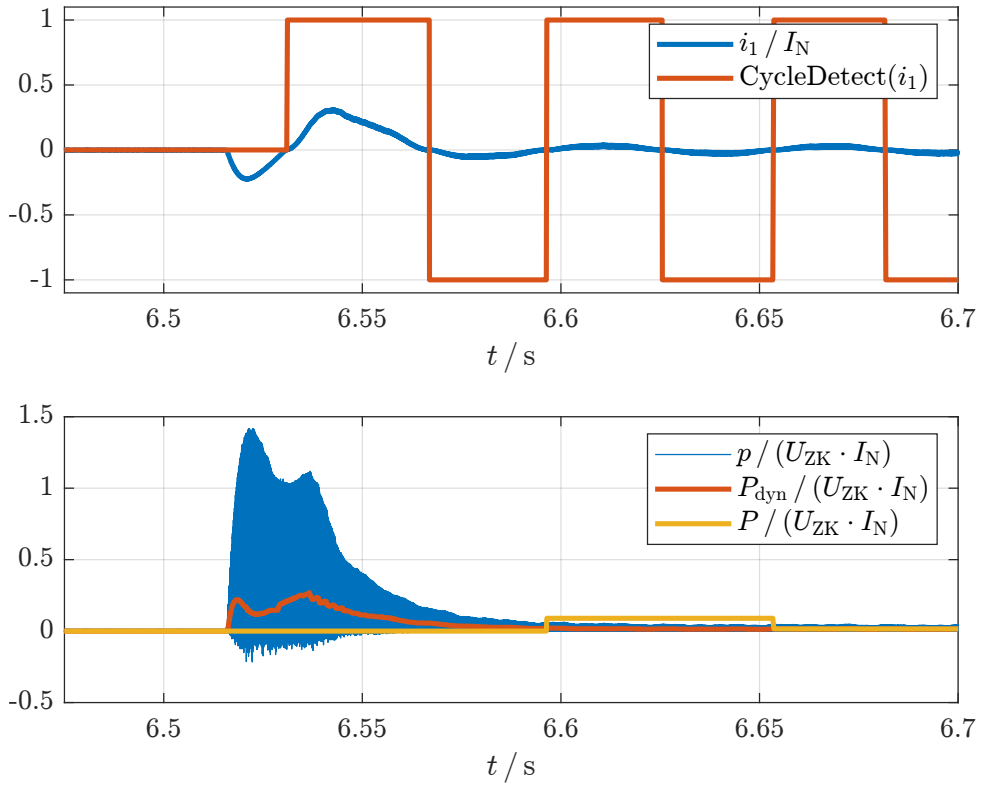

Fig. 6: Instantaneous power $p(t)$, active power P and novel dynamic active power approximation P_{dyn} during a balancing process between two different load operating points with constant speed; $f_{\mathrm{h1}} < 30\,\mathrm{Hz}$, $f_{\mathrm{s}} \approx 16\,\mathrm{kHz}$; [6]

power calculation as an average over the fundamental period. This ensures consistency in the active power data. In addition, knowledge of the fundamental frequency and switching frequency is required anyway for suitable low-pass filtering in order to determine a suitable cut-off frequency of the low-pass filter. This might also need to be adjusted during operation if, for example, the switching frequency changes.

Dynamic transition between different steady state operating points

In the measurement described below, the speed-controlled PMSM is mechanically connected to a torque-controlled load machine in order to be able to investigate different load operating points. Fig. 7 shows the power quantities p, P and P_{dyn}, normalized with regard to the active power P_{AP} related to the investigated motor operating point. The graphic shows two different load operating points including the dynamic transition in between. Initially, the PMSM is driven in generator mode, resulting in negative active power quantities. Then, a load torque step is generated with the torque-controlled load machine by changing both the sign and the magnitude of the torque. This leads to the subsequent motor steady state operation.

As with the previous example, the advantages of switching cycle-based dynamic active power are significant during the transient transition. While the conventional active power P increases stair-wise due to the comparatively long averaging interval of the fundamental period, the dynamic active power even contains the transient peaks and overshoots of the instantaneous power, caused by the inverter control. Furthermore, it can be seen that the two active power quantities show a very high degree of similarity at the respective steady-state operating points.

Conclusively, it can be stated that the dynamic active power P_{dyn} combines the information of the instantaneous power $p(t)$ during transient balancing processes with the information of the conventional active power P during steady state in a novel active power quantity.

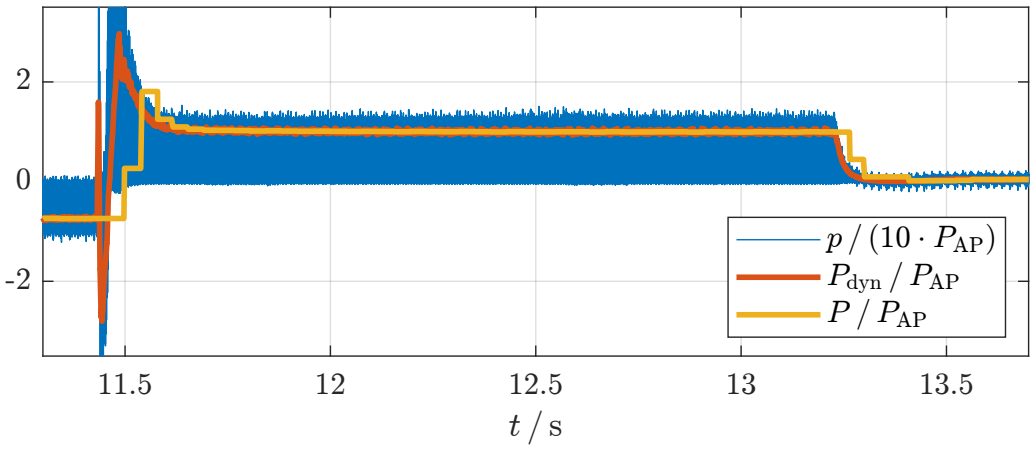

Fig. 7: Instantaneous power $p(t)$, active power P and novel dynamic active power approximation P_{dyn} during a balancing process between two different load operating points with constant speed; $f_{\mathrm{h1}} \approx 20\,\mathrm{Hz}$, $f_{\mathrm{s}} \approx 16\,\mathrm{kHz}$

Accelerated Efficiency Mapping

The commonly known procedure for creating an efficiency map is to measure the device under test (DUT) at different relevant steady-state operating points. In the case of an electric machine, all speed/torque-combinations of interest are approached sequentially and measured under steady state conditions. When a new operating point is invoked, the automation system typically waits until all balancing processes have been completed and the new steady state has been reached. Subsequently, a trigger signal is sent to the measurement system to acquire all relevant physical quantities such as voltages, currents, speed and torque. The electrical and mechanical active powers are then calculated from these measurands individually for each steady state operating point. This procedure can take a long time, especially if there are a large number of operating points to be measured.

If, on the other hand, dynamic power calculation is used, i.e., the active power quantities are determined by averaging over the switching cycle of the inverter, the requirement of a steady state conditions is obsolete. Thus, for each constant speed value, the entire relevant torque range can be passed through in a continuous linear manner. Fig. 8 compares efficiency maps generated using the conventional efficiency mapping process of the PMSM, see Fig. 8a, and one based on the dynamic method, see Fig. 8b. The two measurements were performed separately, but on the same machine from Fig. 5. In Fig. 8a, the stationary speed-torque operating points are marked by the red circles.

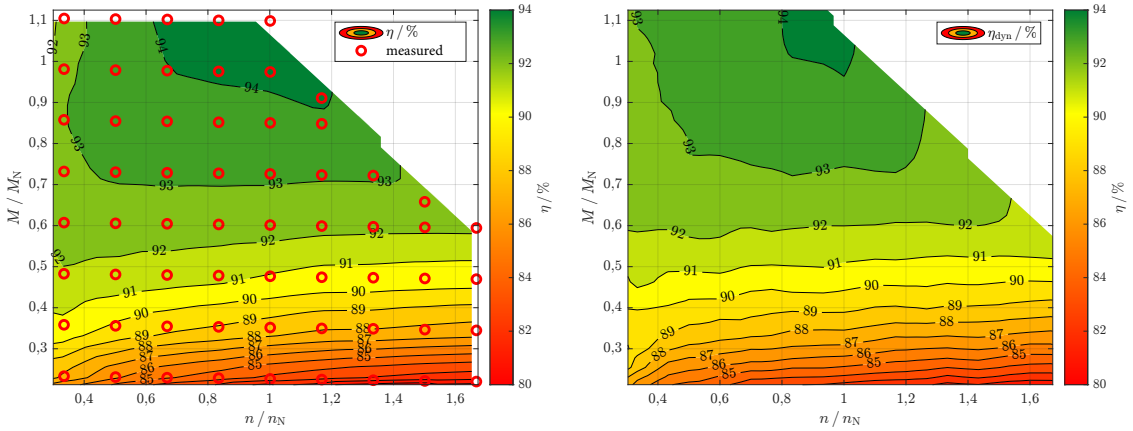

(a) Conventional steady state method [6]

(b) Dynamic evaluation method [6]

Fig. 8: Comparison of a conventional steady state operating point based evaluation and a highly dynamic efficiency mapping method

The deviation of both measurements is less than 0.5 % in most relevant operating points. If a maximum of accuracy is required for the efficiency measurement, then the conventional evaluation during steady state operating points is recommended. However, if a pass-fail test is used to check whether a machine reaches a certain required threshold value of efficiency, the dynamic efficiency mapping is very well suited to generate a meaningful result with drastically reduced measurement duration. During the example measurement in Fig. 8, the required measuring time could be reduced to 10 % of the time needed for the conventional measurement. For reasons of comparability, the dynamic measurement was performed at stationary speeds whereas the torque was increased linearly. However, in general the speed could also be varied continuously. With regard to the automotive application, it is therefore possible to determine the efficiency map as an additional parameter in a Worldwide harmonized Light vehicles Test Procedure (WLTP) that is performed anyway. In doing so, an additional measurement process can be saved. For this reason the dynamic power analysis is very suitable for saving measurement time or even a complete measurement and thus resources and costs, respectively.

Conclusion

This paper presents a method for dynamic real-time power calculation for power meters, which is particularly well suited for highly dynamic applications such as they appear in automotive or robotics. Since the switching period of the power inverter represents the averaging interval of the cycle-based dynamic power quantities, reliable real-time detection of the switching frequency is essential. The presented methodology can be transferred to further cycle-based quantities, such as reactive or apparent power quantities, RMS values, power factor, efficiency, etc. It is very suitable to determine meaningful measurement results even during transient balancing processes in non-stationary operation. Furthermore, this paper presents how this measurement method can be used to perform accelerated efficiency mapping in order to save measuring time and resources in this way. The advantages of the presented method are substantiated by characteristic comparative measurements. Future investigations are concerned with the continuous optimization of real-time switching cycle detection so that it can be flexibly and reliably applied to numerous power inverter topologies.

References

[1] IEC/TS 60034-2-3: Rotating electrical machines – Part 2-3: Specific test methods for determining losses and efficiency of converter-fed AC induction motors. 11/2013.

[2] DIN 40110-1: Wechselstromgrößen Zweileiter-Stromkreise. 03/1994.

[3] DIN 40110-2: Wechselstromgrößen Mehrleiter-Stromkreise. 11/2002.

[4] IEEE Std 1459-2010: IEEE Standard Definitions for the Measurement of Electric Power Quantities Under Sinusoidal, Nonsinusoidal, Balanced, or Unbalanced Conditions. 19. 03. 2010.

[5] Stock, A.; Teigelkötter, J.; Kowalski, T.; Staudt, S.; Ackermans, P.; Lang, K.: Determination of active power on the basis of the switching frequency (Schaltfrequenzbasierte Wirkleistungsmessung). Patent WO 2018/228655 A1. HBM Netherlands B.V. 20. 12. 2018.

[6] Stock, A.: Messtechnische Analyse der Energieverluste von stromrichtergespeisten Antriebssystemen im nichtstationären Betrieb. Dissertation. University of the Federal Armed Forces Munich, 2021.

[7] Stock, A.; Teigelkötter, J.; Staudt, S.; Kowalski, T.: Highly dynamic analysis of active power and fundamental component approximation of inverter fed applications. In: IEEE 12th International Conference on Power Electronics and Drive Systems (PEDS) (Honolulu, USA). IEEE, 2018, pp. 291-296.

[8] Stock, A.; Teigelkötter, J.; Büdel, J.; Staudt, S.: Highly Dynamic Calculation of Power Quantities and Further Analysis of Inverter-Fed Machines. In: 20th European Conference on Power Electronics and Applications (EPE'18 ECCE Europe) (Riga, Latvia). IEEE, 2018.

[9] Depenbrock, M.: The FBD-method, a generally applicable tool for analyzing power relations. In: IEEE Transactions on Power Systems. Vol. 20. no. 2. IEEE, 1993, pp. 381-387.

[10] Staudt, V.: Ein Beitrag zu Leistungsbegriffen und Kompensationsverfahren für Mehrleitersysteme .Habilitation. Ruhr University Bochum, 2000.

[11] Staudt, V.: Fryze – Buchholz – Depenbrock: A time-domain power theory. In: International School on Nonsinusoidal Currents and Compensation 2008 (Łagów, Poland). IEEE, 2008, S. 1-12.

[12] Teigelkötter, J.: Energieeffiziente elektrische Antriebe: Grundlagen, Leistungselektronik, Betriebsverhalten und Regelung von Drehstrommotoren. Springer Vieweg. Wiesbaden, 2013.